Article

Investigation of Floating Offshore Wind Farm Layout Optimization Considering Mooring Line Constraints

Haiying Sun [1,*], Mingdan Li [1], Tianhui Fan [2,*] and Chenzhi Cai [3]

1   School of Marine Science and Engineering, South China University of Technology, Guangzhou 511400, China; 202320163712@mail.scut.edu.cn
2   School of Civil Engineering and Transportation, South China University of Technology, Guangzhou 510640, China
3   School of Civil Engineering, Central South University, Changsha 410083, China; chenzhi.cai@csu.edu.cn
*   Correspondence: sunhaiying@scut.edu.cn or haiying.sun@connect.polyu.hk (H.S.); fanth@scut.edu.cn (T.F.)

Abstract: Floating offshore wind turbines (FOWTs) have become a promising solution for harnessing wind energy in deeper seas. However, the complex interplay between FOWT layout, mooring line patterns, and wake effects significantly influences the overall performance of a floating offshore wind farm (FOWF). This paper proposes a novel optimization methodology that integrates mooring line constraints into the FOWF layout optimization process. The wake-induced power deficit is considered, whereas the vortices are neglected. The new method considers the constraint areas for each FOWT, which are defined based on both mooring line buffer zones and wind turbine buffer zones. By defining constraint areas, the optimization process ensures that FOWTs are optimally positioned while avoiding interference and collisions. By carefully considering the buffer zones, the power potential of FOWFs with three-line, four-line, and six-line mooring configurations can be improved by 122%, 100%, and 78%, respectively. Then, a genetic algorithm is employed to optimize the FOWT positions and mooring line angles simultaneously. The effectiveness of the proposed method is demonstrated through a case study in Guangdong, resulting in a significant 5% increase in power output potential compared to conventional approaches. This research contributes to the advancement of FOWT layout optimization and provides valuable insights for the design and deployment of future FOWFs.

Keywords: floating wind farm; genetic algorithm; mooring pattern; wind farm layout optimization

1. Introduction

The increasing global energy crisis and environmental pollution have spurred significant interest in the development and utilization of clean and renewable energy sources [1]. Wind power, as a clean and sustainable energy source, has experienced significant growth in recent years [2]. To be specific, floating offshore wind turbines (FOWTs) represent a significant advancement in renewable energy technology and have the potential to exploit the vast offshore wind resources in deeper waters. As floating offshore wind farms (FOWFs) increase in size and density, the impact of the wake effect on power generation efficiency becomes increasingly significant [3]. The wake effect, characterized by reduced wind speed and increased turbulence in the downstream region of an operating wind turbine, can lead to substantial power losses, potentially reaching up to 1/3 of the total generated power [4]. For FOWTs, the complex six-degree-of-freedom motions introduce additional complexities to wake dynamics [5], potentially impacting power generation efficiency [6]. For example,

surge motion can contribute to wake recovery downstream of FOWTs [7]. In order to address this challenge, optimizing wind farm layout, such as turbine spacing, arrangement, and orientation, can help mitigate the wake effect, maximize the power output [8], and reduce the total cost of wind energy [9].

Traditional engineering practices prefer regular layouts for ease of construction. However, such layouts can result in significant wake interference and reduce power output in FOWFs. To avoid this problem, careful consideration must be given to the arrangement of turbines. Forinash, et al. [10] introduced an extended pattern search (EPS) approach to optimize wind farm layout, incorporating a cost model, a wake propagation and interaction model, and a wind turbine rotor power model. The optimized wind farm layout is better adapted to the dominant wind direction and can improve the efficiency and economy of power generation. Sun, et al. [11] proposed a novel methodology to simultaneously optimize the size, hub height, and layout of an offshore wind farm. Serrano González, et al. [12] introduced a layout optimization technique tailored for FOWFs equipped with weathervaning turbines. Xu [13] developed an optimization framework utilizing differential evolutionary particle swarm optimization (DPSO) to maximize the power output of FOWFs and pointed out that considering different hub heights can further increase the power output. Liang and Liu [14] proposed a FOWF layout optimization method based on the full-field wake model. The results showed that increasing the number of turbines can achieve a flat peak in power output. Lerch, et al. [15] proposed an adaptive PSO model to optimize FOWF and applied the model to a 500 MW wind farm, achieving a 4.5% reduction in total cost and a 6.4% reduction in energy losses. Hall, et al. [16] proposed a method for optimizing the layout of FOWFs in intricate seabed conditions, in which the influence of wake currents, an inclined seabed, and seabed soil quality were considered. Hietanen, et al. [17] proposed a novel techno-economical layout optimization tool by applying a gradient-free heuristic algorithm to satisfy the engineering and operational constraints in FOWFs. Liang and Liu [18] developed a method for optimizing FOWF layouts with multi-turbine platforms; the method adapts to changing wind conditions by considering the joint distribution of wind speed and wind direction. Tian and Zhong [19] simulated the effects of turbine spacing and the angle between two turbines on the wake field and power of FOWFs. Yilmazlar, et al. [20] studied the layout under mixed rows of fixed-bottom and floating wind turbines using a mixed integer genetic algorithm and found that FOWFs have faster wake recovery and less impact on downstream wind farms compared to their counterpart fixed-bottom offshore wind farms. Wang, et al. [21] used FAST.Farm to study the layout of a hybrid wind farm and showed that placing the FOWFs upstream can improve the overall power output.

In addition to optimizing the spatial arrangement of floating offshore wind turbines, active or passive reposition control techniques can be implemented to reduce the adverse impact of wakes. Rodrigues, et al. [22] proposed a layout optimization framework for FOWFs composed of movable wind turbines, where the outer loop applied an evolutionary algorithm, covariance matrix adaption (CMA-ES), to search for the optimal anchoring position configuration. Similarly, Kheirabadi, et al. [23] repositioned FOWTs by using yaw and axial induction factor adjustment to maximize the power output of the entire wind farm. Froese, et al. [24] proposed an iterative methodology that considered a yaw- and induction-based wind turbine repositioning (YITuR) mechanism to maximize the power output, which allows FOWTs to be passively repositioned according to the wind conditions. Kandemir, et al. [25] proposed a FOWF layout optimization method based on digital twins and dynamic repositioning. In this method, each wind turbine is equipped with a propulsion system and can reposition itself within a constrained area. Mahfouz and Cheng [26] developed a methodology that enables FOWTs to passively adjust their

position by customizing the mooring system according to the wind direction and speed. Niu, et al. [27] proposed a two-level control structure to manipulate the aerodynamic forces acting on the rotating blades of FOWTs, which is achieved by adjusting the control inputs to achieve turbine repositioning. Similarly, Jard and Snaiki [28] equipped FOWTs with a model predictive control (MPC) system which changes the position of the turbines according to the real-time wind conditions. Alkarem, et al. [29] passively repositioned FOWTs by changing the orientation of their mooring lines to reduce the wake effect by as much as 30%. Mahfouz, et al. [30] developed a new mooring system that allows FOWT displacements in a given wind direction, which reduces wake losses by 18% and mooring system material costs by 17%.

Cable configurations significantly impact the electrical layout and cost of wind farms; thus, optimizing cable routes can enhance the overall efficiency of floating wind farms. Poirette, et al. [31] designed an optimization method for array cables of FOWFs by integrating finite element method (FEM) and derivative-free sequential quadratic approximation (SQA) algorithms, which can enhance the performance and economics of FOWFs. Lerch, et al. [32] utilized PSO to optimize the collection grid design of a FOWF, reducing the cost by more than 6% and the energy loss by over 8%. Rapha and Dominguez [33] proposed a suspended cable model to optimize the cable layouts of FOWFs, which can simulate cable configurations and provide key information for the layout optimization.

Recently, shared mooring systems, a novel technology, have emerged as a promising approach to optimizing the layout of floating wind farms by minimizing the number and length of required anchor chains. Building upon previous research on wave energy converter arrays, new solutions to reduce the number of required anchors and moorings through the implementation of shared anchor and mooring systems were proposed by scholars such as Goldschmidt and Muskulus [34] and Fontana, et al. [35]. Later, Hall and Connolly [36] investigated the performance of a square layout of OC4 semi-submersible FOWTs with three distinct sharing approaches. Their research demonstrated that shared mooring systems can maintain acceptable platform motions and exhibit complex recovery behaviors under the influence of wind and wave forces. Wilson, et al. [37] proposed a linearized approach to model shared mooring systems, simplifying the design process and suggesting optimization methods. Their study indicated that a polygonal array layout with vertical anchor positions can maximize system efficiency.

Recent research efforts in FOWF layout optimization have centered on enhancing power generation efficiency and minimizing costs. Strategies such as optimizing layout configurations, dynamically adjusting turbine positions, optimizing cable layouts, and exploring shared mooring systems have been investigated. Nevertheless, the influence of mooring lines on the final layout has received limited attention. This paper addresses this gap by proposing a novel methodology for optimizing FOWT layouts, incorporating mooring line design and layout considerations. Section 1 provides a comprehensive literature review on the FOWT layout optimization problem. Section 2 outlines the underlying assumptions and mooring patterns of this study. Section 3 presents the new methodology and assesses its effectiveness. Section 4 applies the methodology to an actual FOWT case study. Finally, Section 5 summarizes the main conclusions.

2. Definition of Patterns

2.1. Assumption

There are four fundamental assumptions in this study [17]: (a) The inflow wind is steady and uniform in the space; (b) The number of wind turbines is fixed within the wind farm; (c) The area and shape of the wind farm is same for all cases; and (d) All parameters

of wind turbines are identical, including the rotor diameter, the hub height, the rated power, the cut-in wind speed, the rated wind speed, and the cut-out wind speed.

2.2. Mooring Line Footprint Radius

The mooring line footprint is dependent on the specific type of floating platform. This study focuses on semi-submersible floating platforms equipped with catenary mooring lines. To consider the mooring layouts, a simplified catenary equation is employed as a function of water depth D_W to estimate the mooring footprint radius $R_{Mooring}$. The equation is demonstrated as follows [20].

$$R_{Mooring} = \frac{T_H}{\omega} \cosh^{-1}\left(\frac{D_W}{T_H/\omega} + 1\right) \times 1.1 \tag{1}$$

In the equation, T_H is the horizontal design load at the fairlead attachment point. It is calculated by the rated thrust of an NREL 5 MW turbine (ca. 805 kN) multiplied with a safety factor of 2 [38]. w is the mooring line equivalent unit weight in water, which is taken from the OC4 semi-submersible reference design (ca. 1065 N/m) [38]. For the present study, all wind turbines are installed at the same water depth with the same design; therefore, a constant term for T_H/w is assumed for all wind turbines. An additional 10% is added for the mooring line portion lying on the seabed, which is the constant term 1.1 on the right. The relationship of $R_{Mooring}$ and D_W is demonstrated in Figure 1.
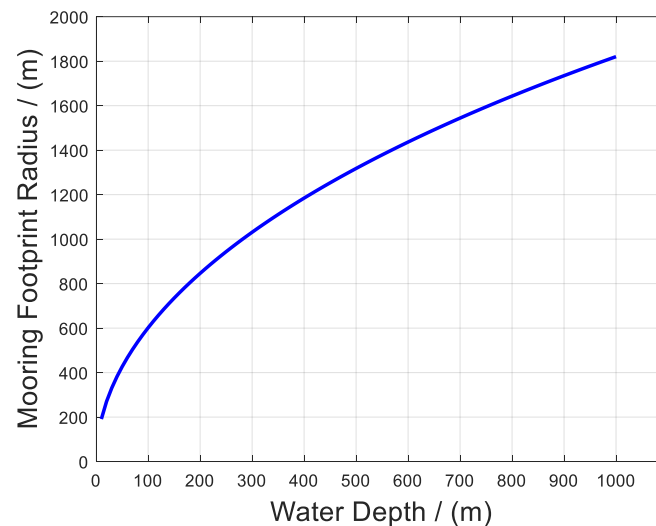

Figure 1. The relationship of the mooring footprint radius and water depth.

2.3. Mooring Line Pattern

Generally, the number of mooring lines should be minimized to keep the most cost-effective design. However, if the required line size for a given number of mooring lines becomes prohibitively large, increasing the number of lines will be necessary. This study investigates three common mooring line patterns: the three-line pattern, the four-line pattern, and the six-line pattern, as demonstrated in Figure 2. For all mooring patterns, the lines are evenly spaced, leading to angles of $120°$, $90°$, and $60°$ between adjacent lines in the three-line pattern, the four-line pattern, and the six-line pattern, respectively.
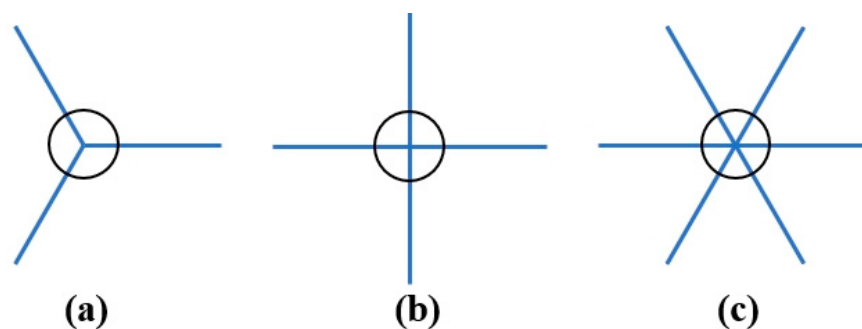
Figure 2. Mooring line patterns: (**a**) three-line pattern; (**b**) four-line pattern; (**c**) six-line pattern. (The black circles represent the wind turbines and the blue lines represent the mooring lines).

3. Methodology

3.1. Constraint Area

Within a wind farm, operating wind turbines can be influenced by wake effects from neighboring turbines. To ensure high power efficiency, the appropriate constraint area is necessary for each wind turbine. The spacing between wind turbines will help reduce the influence caused by wakes within the wind farm. For FOWTs, additional consideration must be given to mooring lines to make sure they are not broken by vessels and machines. In the present study, the comprehensive approach to defining constraint areas for FOWTs considers two aspects, namely, the mooring buffer zone and the wind turbine buffer zone. The spatial boundaries with buffer zones around a FOWT are demonstrated in Figure 3.
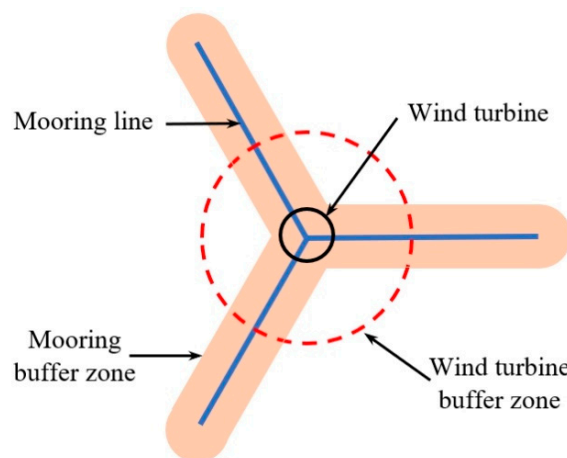

Figure 3. Spatial boundaries around a FOWT.

3.1.1. Mooring Buffer Zone

The mooring buffer zone is an area around each mooring line. In accordance with ISO 19901-7 [39], a minimum separation distance of 100 m between offshore installations is prescribed. Consequently, a 50 m buffer radius around anchors and mooring lines, along with a 100 m safety distance between mooring systems, is considered appropriate [16].

To ensure safety and efficiency of mooring operations, another requirement is that mooring lines must not be crossed within the mooring buffer zone. This will mitigate the increased risks of chafing and unpredictable loading.

3.1.2. Wind Turbine Buffer Zone

The wind turbine buffer zone is defined as an area around each FOWT to ensure operational safety and mitigate wake interference. This zone can be set as a circle, the radius of which should be determined based on the potential variation in wind direction. In

most studies, the minimum distance between wind turbines is set to be 5D (D represents the rotor diameter of wind turbine), so the radius of the buffer zone R_w is 2.5D. It is important to note that no FOWT can be installed in the buffer zones of other FOWTs, but the installation of mooring lines is not prohibited in the area.

The constraint area of each FOWT is subject to the aforementioned buffer zones simultaneously. It is necessary to analyze each buffer zone according to the actual mooring line pattern and rotor diameter. Firstly, the length of mooring line $R_{Mooring}$ should be calculated according to the water depth, and the restricted radius of the wind turbine buffer zone R_w should be calculated based on the rotor size of the target FOWT. Then, these two parameters should be compared to decide the dominant influence factor. If $R_w > R_{Mooring}$, the wind turbine buffer zone encompasses all mooring line areas; therefore, the constraint area is identical to the wind turbine buffer zone. This happens in shallow sea areas. Under this circumstance, the angles of mooring lines can be neglected in the layout optimization process. On the other hand, if $R_w < R_{Mooring}$, the constraint area should be determined by the mooring buffer zone. This happens in deep-sea areas, and the boundary layout in Figure 3 represents this situation. Under this circumstance, the angular orientation of mooring lines should be considered in the layout strategy.

3.2. Optimization Process

FOWT layout optimization is significantly more complex than fixed-bottom wind farm layout optimization. To be specific, factors including the locations of wind turbines, the mooring line pattern, the angles of mooring lines, and the water depth should be considered. Figure 4 illustrates mooring line angles.
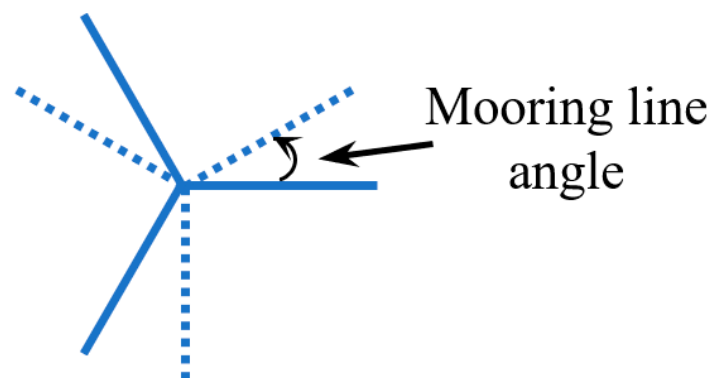

Figure 4. Illustration of mooring line angles.

This study presents a novel method to solve the FOWF layout optimization problem. In the new method, both the positions of FOWTs and the mooring line angles can be optimized simultaneously. The objective is to find the strategy with the maximum power output. The optimization process is as follows, and a flowchart is shown in Figure 5.

Step 1: Initial layout design. Select appropriate FOWT technology (e.g., semi-submersible, tension leg platform) based on water depth, environmental conditions, and project requirements. Determine the mooring line pattern and number of FOWTs based on the size, shape, and specifications of the potential FOWF.

Step 2: Parameterization. Determine the length of the mooring line based on the environmental conditions. Define the x and y coordinates of each FOWT, with mooring line angles as optimization variables. Set the constraint area condition, ensuring sufficient spacing between FOWTs to prevent collisions during operation and maintenance.

Step 3: Optimization problem formulation. Formulate the objective function to maximize the total energy output of the wind farm. Mathematically express all the constraints defined in Step 2.

Step 4: Genetic algorithm (GA) optimization. Apply the GA to the optimization through population initialization, selection, crossover, mutation, and evaluation processes. For each layout strategy, assess its feasibility against the constraint area and eliminate those that do not comply with the specified constraints.

Step 5: Termination criteria and solution selection. Monitor the convergence of the optimization algorithm and terminate when the improvement in the objective function becomes negligible. Repeat the optimization process until the termination criteria is met and the optimized result is obtained.
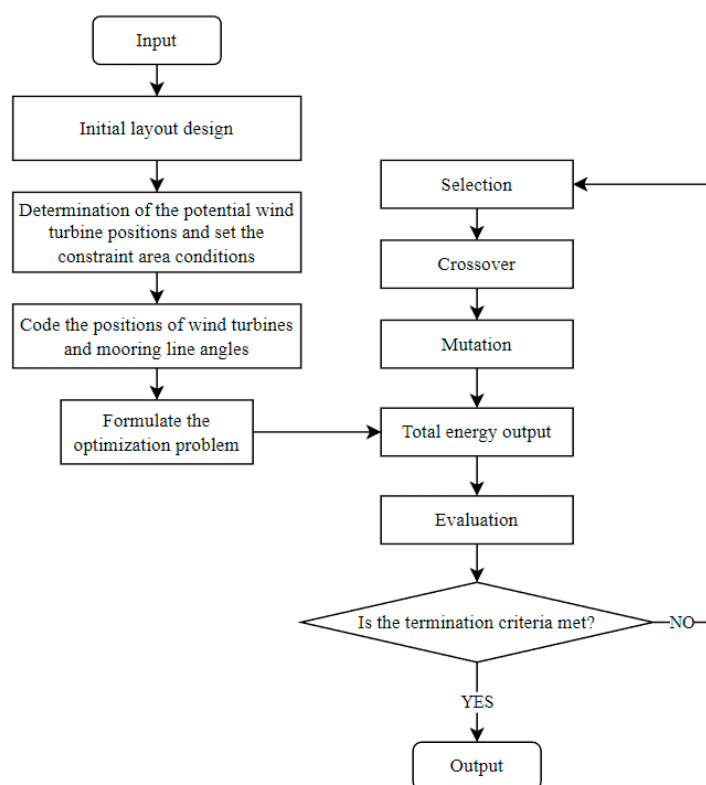

Figure 5. Flowchart of the optimization process.

3.3. Effectiveness

This section evaluates the effectiveness of the proposed optimization method through the comparison of the original strategy and optimized strategies with different mooring line patterns. In all cases, the FOWT model is rated with 10 MW and adopts the three-line mooring layout. Figure 6 demonstrates the original strategy of the FOWF to be optimized. The wind farm is a square with a side length of $30D$. To involve the optimization of the mooring line angle in the strategy, the FOWF is assumed to be installed in a deep-sea area, and $R_{Mooring}$ is assumed to be $5D$. Under this circumstance, the mooring buffer zone dominates the constraint area ($R_w < R_{Mooring}$). In the original layout, the first mooring line is always aligned with the main wave direction at a given site, i.e., all mooring lines are at an angle of $0°$.
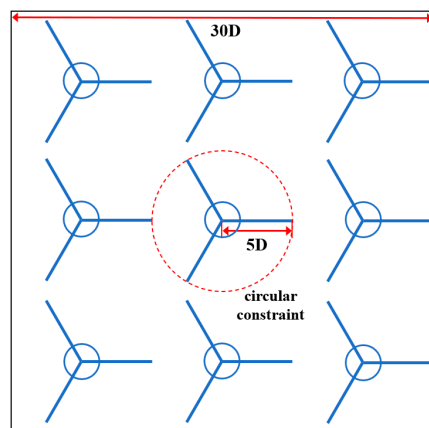
Figure 6. Original strategy of the FOWF (circular constraint).

In this original strategy, a circular constraint is adopted, and the restricted radius is $R_{Mooring}$. A total of nine FOWTs can be installed with a spacing of $10D$ in each direction, so the rated power of this FOWF is 90 MW.

When applying the proposed method, the circular constraint is replaced by the constraint based on the mooring buffer zone. The mooring line angle can be changed in $10°$ intervals. Figure 7 demonstrates the optimized strategy. With this optimization strategy, a total of 20 FOWTs can be installed, and the rated power of this FOWF is 200 MW. Among all FOWTs, twelve of them are at the angle of $10°$, while the other eight are at the angle of $60°$.
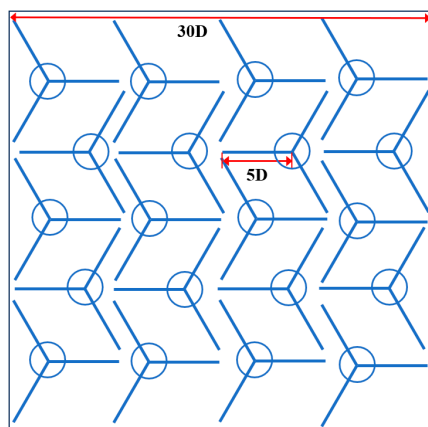

Figure 7. Optimized strategy (three-line layout).

The layout of mooring lines has a significant impact on the power performance of FOWFs as well. Apart from the three-line layout, four-line and six-line layouts are also systematically investigated. Figures 8 and 9 demonstrate the optimized strategies for four-line layouts and six-line layouts, respectively.

Applying the optimization strategy to the four-line layout, a total of 18 FOWTs can be installed, and the rated power of this FOWF is 180 MW. All FOWTs are at an angle of $45°$. While applying the optimization strategy to the six-line layout, a total of 16 FOWTs can be installed, and the rated power of this FOWF is 160 MW. Among all FOWTs, eight of them are at an angle of $0°$, while the other eight are at an angle of $15°$.
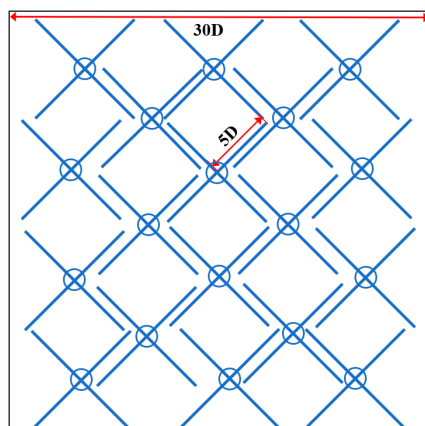
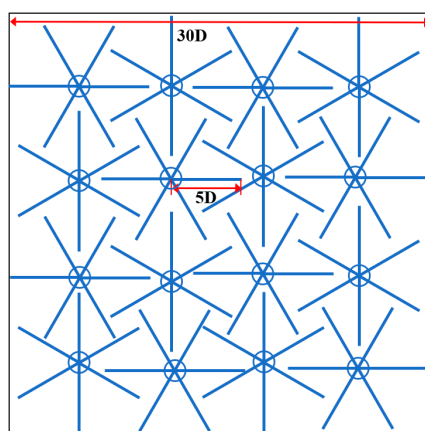**Figure 8.** Optimized strategy (four-line layout).

Figure 9. Optimized strategy (six-line layout).

Comparative analysis of the three layout strategies demonstrates that the proposed method can substantially improve the wind farm power performance, yielding increases of 122%, 100%, and 78%, respectively. Moreover, the mooring line number and pattern significantly impact the available wind farm area as well. The six-line pattern requires the most space, and the three-line pattern can maximize space efficiency. Therefore, by minimizing the number of mooring lines, it is possible to optimize space utilization and enhance the energy yield of the FOWF.

4. Case Study

Subsequent to the evaluation of the proposed FOWT layout optimization method, this section applies the method to a planned offshore wind farm to demonstrate its practical application. The planned offshore wind farm is discussed first. The original wind farm does not consider the mooring layout problem. Then, the proposed method is applied to optimize the layout of the wind farm. The optimized result is compared with the original one, and the effectiveness of the method is analyzed.

4.1. Basic Information

4.1.1. Wind Farm

The planned wind farm is located in the southern sea area of Yangjiang City, Guangdong Province. The wind farm has 73 wind turbines with a total power of 1000 MW. The area of the wind farm is a square with a size of 12 km × 11 km. The layout of the wind

farm is demonstrated in Figure 10. The wind farm is installed in a deep-sea area. Therefore, the constraint area is determined by the mooring buffer zone.
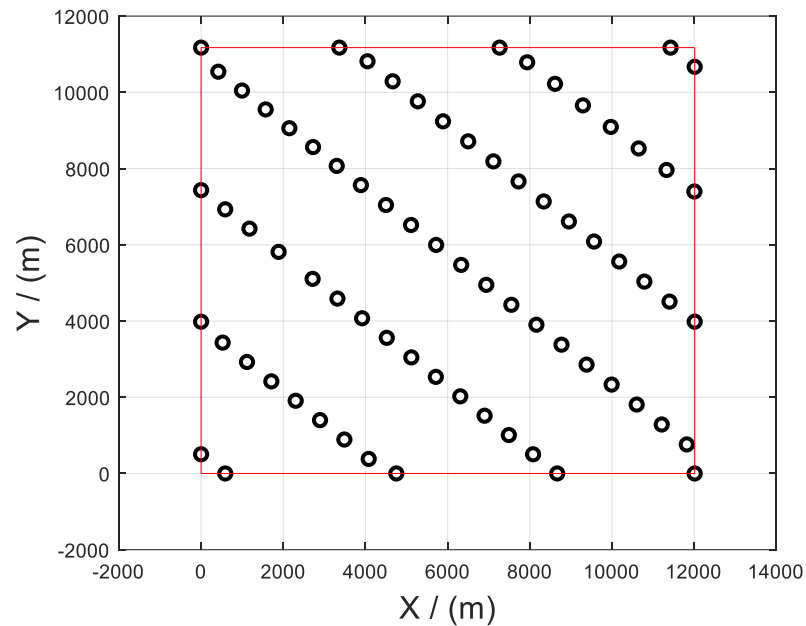

Figure 10. Original wind farm layout. (The red frame is the boundary of the wind farm).

4.1.2. Inflow Wind

The wind speed information is obtained from the two meteorological stations nearest to the site. There are two main wind directions in the area where the wind farm is located, which are northeast and south. The wind shear profile is considered in this study, with the power law profile and an exponent of 0.0680. The annual average wind speed at the hub height is 8.15 m/s, and the turbulence is between 0.076 and 0.119. The wind direction rose measured at the height of 120 m is demonstrated in Figure 11.
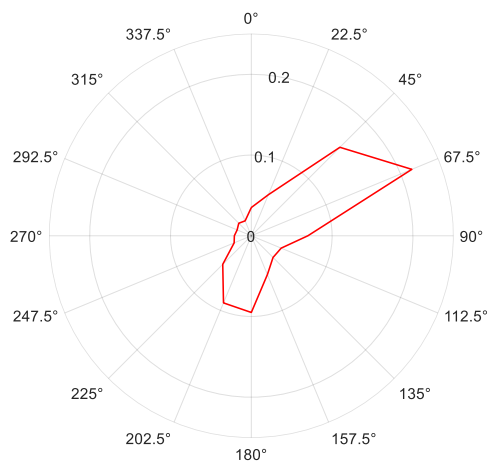

Figure 11. Wind direction rose at the height of 120 m.

4.1.3. Wind Turbine

The wind farm plans to build one type of wind turbine. The rated power of the wind turbine is 14 MW. The parameters of the wind turbine are demonstrated in Table 1.

Table 1. Wind turbine parameters.

Parameter	Value
Rated power	14 MW
Hub height	156 m
Rotor diameter	258 m
Cut-in wind speed	3 m/s
Rated wind speed	12.3 m/s
Cut-out wind speed	25 m/s

4.1.4. Wake Model

The wake effect, characterized by a wind deficit and increased turbulence, is a major problem in wind farm design [40]. The wake generated propagates downstream for a considerable distance, eventually returning to the undisturbed ambient wind [41]. Wake models can describe the spatial distribution of the wind velocity deficit downstream of wind turbines [42]. To be specific, analytical models have more advantages in terms of simplicity and computational speed [43]. To calculate the power loss induced by the wake effect, the Jensen wake model [44] is applied in this study. Since the hub height is 156 m, the wind speed will be converted from 120 m to 156 m according to the power law, and the exponent is introduced in Section 4.1.2.

4.2. Results of Original Layout

To evaluate the effectiveness of each layout, the rated wind speed of 12.3 m/s at the hub height is set as the incoming wind speed in all case studies in this study. For the original wind farm, the power outputs of each wind turbine and the entire wind farm are demonstrated in Figure 12. The red points represent wind turbines, while the number beside the wind turbine is the average power output.
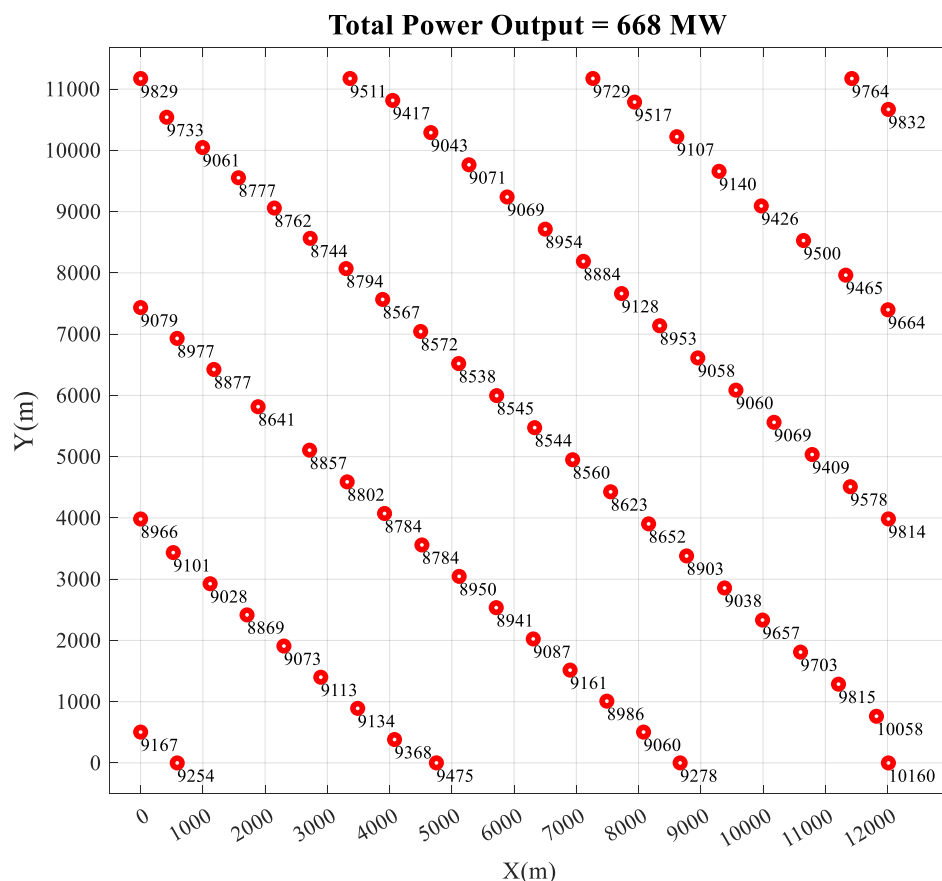

Figure 12. Power output of the original layout.

Due to the wake effect, the total power output of the original wind farm is 668 MW, which is about 67% of the rated power. In the wind farm, the wind turbine at the southeast corner generates the most electricity, with an average power of 10160 MW and an efficiency of 73%. The least efficient wind turbine is located in the middle of the wind farm, with an average power of 8538 MW and an efficiency of 61%. Among all wind turbines, around six wind turbines have an efficiency over 70% (power larger than 9.8 MW), 26 wind turbines have efficiencies between 65% and 70% (power between 9.1 and 9.8 MW), and 41 wind turbines have efficiencies below 65% (power smaller than 9.1 MW). Consequently, this original layout possesses the potential for improving power output.

4.3. Results of Line-Based Restricted Area

In this section, the proposed method is applied to optimize the mooring layout of the wind farm to further improve the efficiency. From the investigation of Section 3.3, the three-line pattern is relatively effective from the perspective of occupied area. Therefore, this study adopts the three-line pattern to optimize the layout of the wind farm. The number of wind turbines is 73; other parameters and the wind information are the same as the original wind farm. The minimum distance between FOWTs is set to be $6D$, so the radius of the buffer zone R_w is $3D$ (774 m). The result of the optimized layout is demonstrated in Figure 13.
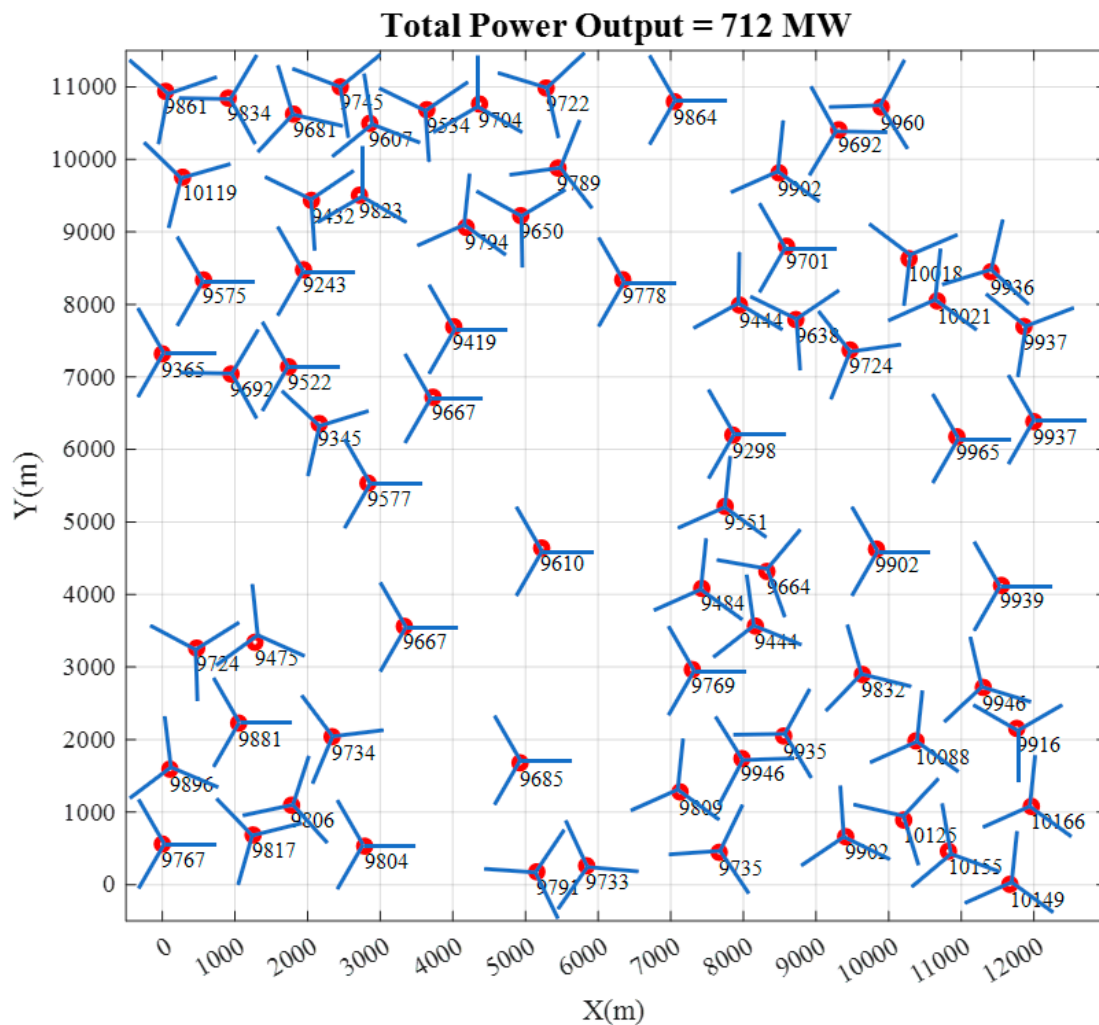

Figure 13. Power output of the optimized layout.

For the optimized layout, the total power output is 712 MW, which is about 71% of the rated power. In the optimized wind farm, the wind turbine with the most power output is also located at the southeast corner, with an average power of 10,155 MW and an efficiency of 73%. The least efficient wind turbine is located in the west of the wind farm, with an average power of 9243 MW and an efficiency of 66%. Among all wind turbines, around 32 wind turbines have an efficiency over 70% (power larger than 9.8 MW), and 41 wind turbines have an efficiency below 66% (power smaller than 9.8 MW). A key finding from this case study is that optimizing mooring line angles presents a significant opportunity to save wind farm area and maximize overall power output.

4.4. Comparison

Compared with the original layout, the optimization method improves the total power from 668 MW to 712 MW, and the efficiency reaches more than 71%. The obvious impact lies in the decrease in the number of low-power wind turbines. In the optimized layout, all wind turbines have efficiencies over 66%, which is much higher than the 61% of the original wind farm. Considering the power difference between the largest and least powerful wind turbines, the original wind farm produces 1622 MW, while the optimized wind farm produces 912 MW, which means more wind turbines reach their largest potential. Therefore, the proposed optimization method can significantly improve the power output of the FOWF.

5. Conclusions

This paper introduces a novel optimization approach for a floating offshore wind turbine (FOWT) layout that incorporates constraints on mooring line patterns, thereby improving the overall performance and efficiency of the floating offshore wind farm (FOWF). A systematic investigation into the influence of mooring line patterns on the FOWT layout was conducted to validate the proposed approach. The conclusions of this paper can be summarized as follows:

(1)   A comprehensive literature review on the FOWF layout optimization problem was conducted. Current studies predominantly concentrate on maximizing power generation efficiency and minimizing costs. The common techniques include layout optimization, dynamic wind turbine positioning, cable layout optimization, and shared mooring systems. Nevertheless, the influence of mooring lines on the optimized layout has not been sufficiently explored and requires further attention.

(2)   An in-depth analysis of FOWT mooring line patterns was presented. The footprint radius of mooring lines was calculated considering water depth, and the number of lines was determined based on load and size constraints. Three representative mooring line patterns were subsequently introduced and investigated in detail.

(3)   A novel FOWF layout optimization process was presented in this study. The constraint area for each FOWT was defined by incorporating both a mooring line buffer zone and a wind turbine buffer zone, with the constraint strategy dynamically adjusted based on water depth. A genetic algorithm was employed as the optimization tool. The proposed method was evaluated through a comparative analysis of three representative mooring line patterns. Results demonstrated a substantial increase in power output potential within the specified FOWT area, highlighting the effectiveness of the proposed optimization framework.

(4)   The proposed FOWF layout optimization method was applied to a case study in Guangdong. The optimization process considered both FOWT positions and mooring line angles simultaneously. The results indicated a significant improvement in power

output potential, from 66% to 71%, highlighting the effectiveness of the proposed method for FOWF configuration design.

In conclusion, careful consideration of practical factors is crucial for the successful design of FOWF systems. This study demonstrates the potential for significant power efficiency gains (up to 5%) by optimizing FOWT positions and mooring line angles. Future research should expand upon these findings by investigating the influence of additional factors, such as seabed terrain, mooring line materials, and anchor types, on the optimal layout and performance of FOWF arrays.

Author Contributions: Conceptualization, H.S. and T.F.; Methodology, H.S.; Software, H.S.; Validation, H.S. and T.F.; Writing–original draft, H.S. and M.L.; Writing—review & editing, C.C.; Project administration, T.F.; Resources, T.F.; Supervision, T.F. All authors have read and agreed to the published version of the manuscript.

Institutional Review Board Statement: Not applicable.

Informed Consent Statement: Not applicable.

Data Availability Statement: The original contributions presented in the study are included in the article, further inquiries can be directed to the corresponding authors.

Conflicts of Interest: The authors declare no conflict of interest.

Abbreviations

Nomenclature

D	Rotor diameter of wind turbine
D_W	Water depth
$R_{Mooring}$	Mooring footprint radius
R_w	Radius of the buffer zone
T_H	Horizontal design load at the fairlead attachment point
w	Mooring line equivalent unit weight in water

Abbreviation

CMA-ES	Covariance matrix adaption
DPSO	Differential evolutionary particle swarm optimization
EPS	Extended pattern search
GA	Genetic algorithm
FEM	Finite element method
FOWF	Floating offshore wind farm
FOWT	Floating offshore wind turbine
MPC	Model predictive control
SQA	Sequential quadratic approximation
YITuR	Yaw- and induction-based wind turbine repositioning

References

1. Yalew, S.G.; van Vliet, M.T.H.; Gernaat, D.E.H.J.; Ludwig, F.; Miara, A.; Park, C.; Byers, E.; De Cian, E.; Piontek, F.; Iyer, G.; et al. Impacts of climate change on energy systems in global and regional scenarios. *Nat. Energy* **2020**, *5*, 794–802. [CrossRef]
2. Sun, H.; Yang, H.; Gao, X. Investigation into spacing restriction and layout optimization of wind farm with multiple types of wind turbines. *Energy* **2019**, *168*, 637–650. [CrossRef]
3. Akhtar, N.; Geyer, B.; Rockel, B.; Sommer, P.S.; Schrum, C. Accelerating deployment of offshore wind energy alter wind climate and reduce future power generation potentials. *Sci. Rep.* **2021**, *11*, 11826. [CrossRef]
4. Pryor, S.C.; Barthelmie, R.J.; Shepherd, T.J. Wind power production from very large offshore wind farms. *Joule* **2021**, *5*, 2663–2686. [CrossRef]
5. Tomasicchio, G.; Avossa, A.M.; Riefolo, L.; Ricciardelli, F.; Musci, E.; D'Alessandro, F.; Vicinanza, D. Dynamic Modelling of a Spar Buoy Wind Turbine. In Proceedings of the ASME 2017 36th International Conference on Ocean, Offshore and Arctic Engineering, Trondheim, Norway, 25–30 June 2017. [CrossRef]
6. Kim, H.; Han, W.; Kim, D.; Lee, S. Windfarm layout optimization with a newly-modified multi-wake model based on aerodynamic characteristics of floating wind-turbines. *J. Mech. Sci. Technol.* **2023**, *37*, 4661–4670. [CrossRef]
7. Alkhabbaz, A.; Hamza, H.; Daabo, A.M.; Yang, H.-S.; Yoon, M.; Koprulu, A.; Lee, Y.-H. The aero-hydrodynamic interference impact on the NREL 5-MW floating wind turbine experiencing surge motion. *Ocean Eng.* **2024**, *295*, 116970. [CrossRef]
8. Choi, E.H.; Cho, J.R.; Lim, O.K. Layout optimization for multi-platform offshore wind farm composed of spar-type floating wind turbines. *Wind Struct.* **2015**, *20*, 751–761. [CrossRef]
9. Sun, H.; Gao, X.; Yang, H. A review of full-scale wind-field measurements of the wind-turbine wake effect and a measurement of the wake-interaction effect. *Renew. Sustain. Energy Rev.* **2020**, *132*, 110042. [CrossRef]
10. Forinash, C.; DuPont, B. An extended pattern search method for offshore floating wind layout and turbine geometry optimization. In Proceedings of the ASME 2016 International Design Engineering Technical Conferences and Computers and Information in Engineering Conference, Charlotte, NC, USA, 21–24 August 2016.
11. Sun, H.; Yang, H.; Tao, S. Optimization of the Number, Hub Height and Layout of Offshore Wind Turbines. *J. Mar. Sci. Eng.* **2023**, *11*, 1566. [CrossRef]
12. Serrano González, J.; Burgos Payán, M.; Riquelme Santos, J.M.; González Rodríguez, Á.G. Optimal Micro-Siting of Weathervaning Floating Wind Turbines. *Energies* **2021**, *14*, 886. [CrossRef]
13. Xu, X. Extreme Response Analysis of a Site-Specific Offshore Wind Turbine and Offshore Wind Farm Offshore Wind Farm Layout Optimization. Doctoral Dissertation, Florida Institute of Technology, Melbourne, FL, USA, 2020.
14. Liang, Z.; Liu, H. Layout Optimization of a Modular Floating Wind Farm Based on the Full-Field Wake Model. *Energies* **2022**, *15*, 809. [CrossRef]
15. Lerch, M.; De-Prada-Gil, M.; Molins, C. A metaheuristic optimization model for the inter-array layout planning of floating offshore wind farms. *Int. J. Electr. Power Energy Syst.* **2021**, *131*, 107128. [CrossRef]
16. Hall, M.; Biglu, M.; Housner, S.; Coughlan, K.; Mahfouz, M.Y.; Lozon, E. Floating Wind Farm Layout Optimization Considering Moorings and Seabed Variations. *J. Phys. Conf. Ser.* **2024**, *2767*, 062038. [CrossRef]
17. Hietanen, A.I.; Snedker, T.H.; Dykes, K.; Bayati, I. A novel techno-economical layout optimization tool for floating wind farm design. *Wind Energ. Sci.* **2024**, *9*, 417–438. [CrossRef]
18. Liang, Z.; Liu, H. Layout optimization of an offshore floating wind farm deployed with novel multi-turbine platforms with the self-adaptive property. *Ocean Eng.* **2023**, *283*, 115098. [CrossRef]
19. Tian, Y.; Zhong, Y. Effects of turbine layout spacing and angle on wake interference of floating offshore wind farms. *J. Mech. Sci. Technol.* **2024**, *38*, 1237–1248. [CrossRef]
20. Yilmazlar, K.; White, C.; Cacciola, S.; Candido, J.; Croce, A. Floating wind farm design using social and environmental constraints. *J. Phys. Conf. Ser.* **2024**, *2767*, 092081. [CrossRef]
21. Wang, K.; Chen, S.; Chen, J.; Zhao, M.; Lin, Y. Study on wake characteristics of fixed wind turbines and floating wind turbines arranged in tandem. *Ocean Eng.* **2024**, *304*, 117808. [CrossRef]
22. Rodrigues, S.F.; Pinto, R.T.; Soleimanzadeh, M.; Bosman, P.A.N.; Bauer, P. Wake losses optimization of offshore wind farms with moveable floating wind turbines. *Energy Convers. Manag.* **2015**, *89*, 933–941. [CrossRef]
23. Kheirabadi, A.C.; Nagamune, R. Modeling and Power Optimization of Floating Offshore Wind Farms with Yaw and Induction-based Turbine Repositioning. In Proceedings of the American Control Conference (ACC), Philadelphia, PA, USA, 10–12 July 2019; pp. 5458–5463.
24. Froese, G.; Ku, S.Y.; Kheirabadi, A.C.; Nagamune, R. Optimal layout design of floating offshore wind farms. *Renew. Energy* **2022**, *190*, 94–102. [CrossRef]
25. Kandemir, E.; Liu, J.; Hasan, A. Digital twin-driven dynamic repositioning of floating offshore wind farms. *Energy Rep.* **2023**, *9*, 208–214. [CrossRef]

26. Mahfouz, M.Y.; Cheng, P.-W. A passively self-adjusting floating wind farm layout to increase the annual energy production. *Wind Energy* **2023**, *26*, 251–265. [CrossRef]

27. Niu, Y.; Lathi, P.P.; Nagamune, R. Floating Offshore Wind Farm Control via Turbine Repositioning with Aerodynamic Force. In Proceedings of the American Control Conference (ACC), San Diego, CA, USA, 31 May–2 June 2023; pp. 2542–2547.

28. Jard, T.; Snaiki, R. Real-Time Dynamic Layout Optimization for Floating Offshore Wind Farm Control. *Ocean. Eng.* **2025**, *316*, 119971. [CrossRef]

29. Alkarem, Y.R.; Huguenard, K.; Verma, A.S.; Van Binsbergen, D.; Bachynski-Polic, E.; Nejad, A.R. Passive Mooring-based Turbine Repositioning Technique for Wake Steering in Floating Offshore Wind Farms. *J. Phys. Conf. Ser.* **2024**, *2767*, 092056. [CrossRef]

30. Mahfouz, M.Y.; Lozon, E.; Hall, M.; Cheng, P.W. Integrated floating wind farm layout design and mooring system optimization to increase annual energy production. *J. Phys. Conf. Ser.* **2024**, *2767*, 062020. [CrossRef]

31. Poirette, Y.; Guiton, M.; Huwart, G.; Sinoquet, D.; Leroy, J.M. An Optimization Method for the Configuration of Inter Array Cables for Floating Offshore Wind Farm. In Proceedings of the ASME 2017 36th International Conference on Ocean, Offshore and Arctic Engineering, Trondheim, Norway, 25–30 June 2017; Volume 10. [CrossRef]

32. Lerch, M.; De-Prada-Gil, M.; Molins, C. Collection Grid Optimization of a Floating Offshore Wind Farm Using Particle Swarm Theory. In Proceedings of the 16th Deep Sea Offshore Wind R and D Conference (EERA DeepWind), SINTEF, Trondheim, Norway, 16–18 January 2019; Volume 1356. [CrossRef]

33. Rapha, J.I.; Dominguez, J.L. Suspended cable model for layout optimisation purposes in floating offshore wind farms. In Proceedings of the European-Energy-Research-Alliance (EERA) 18th Deep Sea Offshore Wind R and D Digital Conference (EERA DeepWind), Sintef, Electr Network, Trondheim, Norway, 13–15 January 2021; Volume 2018. [CrossRef]

34. Goldschmidt, M.; Muskulus, M. Coupled Mooring Systems for Floating Wind Farms. *Energy Procedia* **2015**, *80*, 255–262. [CrossRef]

35. Fontana, C.M.; Arwade, S.R.; DeGroot, D.J.; Myers, A.T.; Landon, M.; Aubeny, C. Efficient Multiline Anchor Systems for Floating Offshore Wind Turbines. In Proceedings of the ASME 2016 35th International Conference on Ocean, Offshore and Arctic Engineering, Busan, Republic of Korea, 19–24 June 2016; Volume 6. [CrossRef]

36. Hall, M.; Connolly, P. Coupled Dynamics Modelling of a Floating Wind Farm with Shared Mooring Lines. In Proceedings of the ASME 2018 37th International Conference on Ocean, Offshore and Arctic Engineering, Madrid, Spain, 17–22 June 2018.

37. Wilson, S.; Hall, M.; Housner, S.; Sirnivas, S. Linearized modeling and optimization of shared mooring systems. *Ocean Eng.* **2021**, *241*, 110009. [CrossRef]

38. Robertson, A.; Jonkman, J.; Masciola, M.; Song, H.; Goupee, A.; Coulling, A.; Luan, C. *Definition of the Semisubmersible Floating System for Phase II of OC4*; National Renewable Energy Laboratory: Golden, CO, USA, 2014.

39. *ISO 19901-7:2013*; Petroleum and Natural Gas Industries—Specific Requirements for Offshore Structures. ISO: Geneva, Switzerland, 2013.

40. Sun, H.; Qiu, C.; Lu, L.; Gao, X.; Chen, J.; Yang, H. Wind turbine power modelling and optimization using artificial neural network with wind field experimental data. *Appl. Energy* **2020**, *280*, 115880. [CrossRef]

41. Sun, H.; Yang, H. Study on an innovative three-dimensional wind turbine wake model. *Appl. Energy* **2018**, *226*, 483–493. [CrossRef]

42. Du, B.; Ge, M.; Li, X.; Liu, Y. A momentum-conserving wake superposition method for wind-farm flows under pressure gradient. *J. Fluid Mech.* **2024**, *999*, A27. [CrossRef]

43. Sun, H.; Yang, H. Numerical investigation of the average wind speed of a single wind turbine and development of a novel three-dimensional multiple wind turbine wake model. *Renew. Energy* **2020**, *147*, 192–203. [CrossRef]

44. Jensen, N.O. A Note on Wind Generator Interaction. 1983. Available online: https://backend.orbit.dtu.dk/ws/portalfiles/portal/55857682/ris_m_2411.pdf (accessed on 28 December 2024).